Influence of Non-Homogeneous Foundations On the Dynamic Responses of Railway Sleepers

Le-Hung Tran, Tien Hoang, Denis Duhamel, Gilles Forêt, Samir Messad, Arnaud Loaëc

Accepted Manuscript

International Journal of Structural Stability and Dynamics

Article Title:	Influence of non-homogeneous foundations on the dynamic responses of railway sleepers
Author(s):	Le-Hung Tran, Tien Hoang, Denis Duhamel, Gilles Foret, Samir Messad, Arnaud Loaec
DOI:	10.1142/S0219455421500024
Received:	20 April 2020
Accepted:	27 August 2020
To be cited as:	Le-Hung Tran *et al.*, Influence of non-homogeneous foundations on the dynamic responses of railway sleepers, *International Journal of Structural Stability and Dynamics*, doi: 10.1142/S0219455421500024
Link to final version:	https://doi.org/10.1142/S0219455421500024

International Journal of Structural Stability and Dynamics

Influence of non-homogeneous foundations on the dynamic responses of railway sleepers

Le-Hung Tran*
Laboratoire Navier, École des Ponts ParisTech
Université Gustave Eiffel, CNRS
77420, Champs-sur-Marne, France
le-hung.tran@enpc.fr

Tien Hoang
Laboratoire Navier, École des Ponts ParisTech
Université Gustave Eiffel, CNRS
77420, Champs-sur-Marne, France
tien.hoang@enpc.fr

Denis Duhamel
Laboratoire Navier, École des Ponts ParisTech
Université Gustave Eiffel, CNRS
77420, Champs-sur-Marne, France
denis.duhamel@enpc.fr

Gilles Foret
Laboratoire Navier, École des Ponts ParisTech
Université Gustave Eiffel, CNRS
77420, Champs-sur-Marne, France
gilles.foret@enpc.fr

Samir Messad
Sateba, Consolis Group
Courbevoie, 92400, France
s.messad@sateba.com

Arnaud Loaëc
Sateba, Consolis Group
Courbevoie, 92400, France
a.loaec@sateba.com

Received (Day Month Year)
Accepted (Day Month Year)

In a railway track, the sleeper's responses on a non-homogeneous foundation have been investigated by researchers focusing on the foundation behavior along the rails. However, the foundation can also vary along the sleeper length, particularly when the track is newly tamped. The foundation at the sleeper center is often weaker than those under

*Corresponding author.

the rails and this non-homogeneity directly affects the sleeper responses. This paper presents a new model to calculate the influence of such foundations on the dynamic responses of the railway sleepers. This model is developed by combining a finite element model for the sleepers and foundation and a model of periodically supported beams subjected to moving loads for the rails. In this paper, the foundation contains three parts with different mechanical behaviors. The sleeper's responses can be calculated by transforming the finite-element dynamic stiffness matrix to the one considering the boundary conditions and the relation between the rail seat forces and rail displacements governed by the beam model. This method reduces all the degrees of freedom of the railway track to its one period which gives a substantial reduction in computational time. The numerical applications show that the more homogeneous (so-called consolidated) the foundation is, the larger the sleeper strain is at its center. This result shows the potential application of the sleeper responses to estimating the consolidation level of the foundation.

Keywords: Railway; sleeper; non-homogeneous foundation; semi-analytic method; consolidated ballast.

1. Introduction

Railway sleepers are transverse beams laying on ballast to support and secure the rails, providing safe navigation of rolling stock. In this article, we study the influence of the foundation on the dynamic responses of sleeper. We consider that the foundation behavior varies along the sleeper length as shown in the Fig. 1.[1] When the track is tamped, the part of the ballast inside the two rails is normally less stiff than that at the rail positions. Over time, the ballast deteriorates, the middle part is densified and its stiffness increases (so-called the cosolidated ballast). By studying the sleeper responses in difference cases, we can deduce the evolution of ballast/foundation.

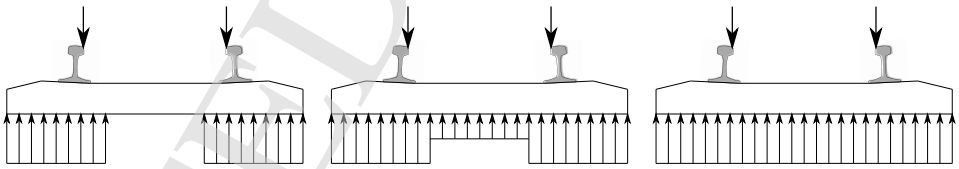

(a) Newly tamped (b) Partially consolidation (c) Homogeneous

Fig. 1: Evolution of railway foundation

For this purpose, we have developed an semi-analytical model for a railway track. There are numerous models for the mechanical behaviors of railway tracks. Among these methods, the most widely used are the analytical methods based on a beam posed on a homogeneous foundation[2–7] or a periodically supported beam.[8–11] However, these methods are limited to simple foundation models such as Winkler or Kelvin-Voigt foundation. Non-linear foundations have been studied by different techniques. Ding et al.[12] used a Runge-Kutta method to calculate the dynamic responses of a beam on a nonlinear foundation. The importance of non-linearity

September 1, 2020 9:51 IJSSD-D-20-00185

of the track support system on the overall behavior has been demonstrated by Sadeghi and Fesharaki.[13] In this work, the track response was calculated at any time step from the responses obtained for the previous step by an iteration method which is presented by Morino et al.[14] In 2016, Hoang et al.[15] used a harmonic balance method for periodically supported beams on a nonlinear foundation. Recently, Yang et al.[16] developed an explicit periodic nonlinear model for damaged foundations which has been validated by FEM methods and the in-situ measurements. In order to take into account the non-homogeneous nature of the track substructure, the finite element method has been used in numerous studies.[17–26] This method is particularly useful to study the sleeper frequencies.[27–30] By coupling an analytical and numerical model, Gustavson and Gylltoft[31] studied the influence of crack sleepers on a track response. Ruiz et al.[32] used the same method to calculate track responses by an implicit iteration. One limitation of the numerical methods is that the dimensions of track components are not of the same scale (the rails are longer than the sleeper and the dimension of foundation is much bigger than ones of sleepers, rail pads and rails). This problem generates numerous degrees of freedom of the railway track and it significantly increases computing time. Some studies have been developed to reduce the number of degrees of freedom by different techniques. The semi-analytical model has been shown to be a good approach for this type of problem.[33]

The proposed model is based on the finite element method for the sleepers together with the foundation and an analytical model for the rails and the rail pads. The foundation consists of three parts with different mechanical behaviors to model the non-homogeneity. By substituting the boundary condition of the foundation into the dynamic equation of the FEM model, we obtain the first relation between the rail seats displacements and forces. On the other side, we have the second relation between these displacements and forces from the analytical model applying each rail subjected to moving loads.[34] By combining these two relations, the sleeper response can be calculated in the frequency domain and then the time domain. The numerical applications show the coherence between the numerical and analytical models in the case of homogeneous foundations. In the case of non-homogeneous foundation, the results show that when the foundation is more consolidated, the strain is more important at the sleeper center. Moreover, we have studied the sleeper response when the loads are unequal at the two rails.

2. Formulations

Let us consider a railway track with a sleeper posed on a visco-elastic foundation as shown in Fig. 2a. In this figure, the rail is modeled as an infinite beam subjected to moving loads using the Euler-Bernoulli's beam model (this model is presented in Appendix B). We will compute the dynamic responses of the sleepers by considering only one period of the track as shown in Fig. 2b.

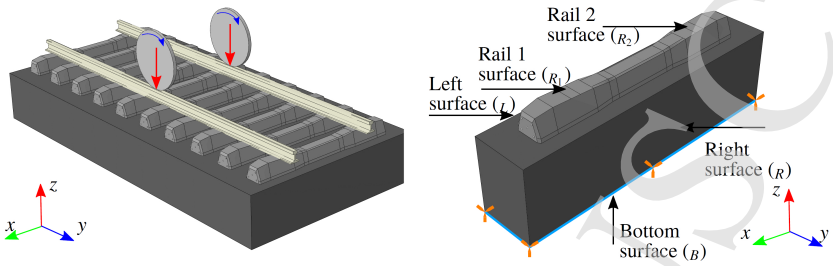

(a) Railway track in 3D

(b) Numerical model of the sleeper and foundation

Fig. 2: Coupling of analytical and numerical models

By using FEM, we obtain the dynamic equation of the substructure as follows:

$$\mathbf{M}\ddot{\mathbf{u}}(t) + \mathbf{C}\dot{\mathbf{u}}(t) + \mathbf{K}\mathbf{u}(t) = \mathbf{F}(t) \tag{2.1}$$

where $\mathbf{M}$, $\mathbf{C}$ and $\mathbf{K}$ are the mass, damping and stiffness matrices of the sleeper and foundation respectively, $\mathbf{u}(t)$ and $\mathbf{F}(t)$ are the nodal displacements and forces in the time domain. ($\dot{\square}$) denotes the partial derivative with respect to time. By using the Fourier transform, Eq. (2.1) can be rewritten in the frequency domain as follows:

$$\mathbf{D}(\omega)\hat{\mathbf{u}}(\omega) = \hat{\mathbf{F}}(\omega) \tag{2.2}$$

where ω is the angular velocity and

$$\mathbf{D}(\omega) = -\omega^2\mathbf{M} + \mathrm{i}\omega\mathbf{C} + \mathbf{K} \tag{2.3}$$

We denote that the index $_L$, $_R$, $_B$, $_{R_1}$, $_{R_2}$ and $_I$ represent respectively the degrees of freedom (DOF) of the foundation and sleeper at the left boundary, at the right boundary, at the bottom boundary, contact surface rail 1 boundary, contact surface rail 2 boundary and the others (see Fig 2b). By taking into account the boundary condition at the base $\hat{\mathbf{u}}_B = \mathbf{0}$ and no force density at the interior nodes ($\hat{\mathbf{F}}_I = \mathbf{0}$), Eq. (2.2) can be rewritten as follows:

$$\begin{bmatrix} \mathbf{D}_{R_1R_1} & \mathbf{D}_{R_1R_2} & \mathbf{D}_{R_1L} & \mathbf{D}_{R_1R} & \mathbf{D}_{R_1I} \\ \mathbf{D}_{R_2R_1} & \mathbf{D}_{R_2R_2} & \mathbf{D}_{R_2L} & \mathbf{D}_{R_2R} & \mathbf{D}_{R_2I} \\ \mathbf{D}_{LR_1} & \mathbf{D}_{LR_2} & \mathbf{D}_{LL} & \mathbf{D}_{LR} & \mathbf{D}_{LI} \\ \mathbf{D}_{RR_1} & \mathbf{D}_{RR_2} & \mathbf{D}_{RL} & \mathbf{D}_{RR} & \mathbf{D}_{RI} \\ \mathbf{D}_{IR_1} & \mathbf{D}_{IR_2} & \mathbf{D}_{IL} & \mathbf{D}_{IR} & \mathbf{D}_{II} \end{bmatrix} \begin{bmatrix} \hat{\mathbf{u}}_{R_1} \\ \hat{\mathbf{u}}_{R_2} \\ \hat{\mathbf{u}}_L \\ \hat{\mathbf{u}}_R \\ \hat{\mathbf{u}}_I \end{bmatrix} = \begin{bmatrix} \hat{\mathbf{F}}_{R_1} \\ \hat{\mathbf{F}}_{R_2} \\ \hat{\mathbf{F}}_L \\ \hat{\mathbf{F}}_R \\ \mathbf{0} \end{bmatrix} \tag{2.4}$$

In the steady-state, we suppose that the responses of the track period are unchanged when the moving forces come and leave this interval but with a delay which is equal to the time for the force to cover the length of the track interval (so-called the steady-state condition):

$$\begin{cases} \mathbf{u}_R(t) = \mathbf{u}_L\left(t + \dfrac{L}{v}\right) \\ \mathbf{F}_R(t) = -\mathbf{F}_L\left(t + \dfrac{L}{v}\right) \end{cases} \tag{2.5}$$

September 1, 2020 9:51 IJSSD-D-20-00185

where L and v are the length of the interval and moving force speed respectively. By using the Fourier transform, Eq. (2.5) can be rewritten as follows:

$$\begin{cases} \hat{\mathbf{u}}_R = \hat{\mathbf{u}}_L \mathrm{e}^{\left(\frac{\mathrm{i}\omega L}{v}\right)} \\ \hat{\mathbf{F}}_R = -\hat{\mathbf{F}}_L \mathrm{e}^{\left(\frac{\mathrm{i}\omega L}{v}\right)} \end{cases} \tag{2.6}$$

By substituting the Eq. (2.6) into Eq. (2.4) and transforming the rows and columns of the dynamic stiffness matrix, we can obtain the following result (the detail is shown in Appendix A):

$$\begin{bmatrix} \mathbf{D}_{R_1R_1} & \mathbf{D}_{R_1R_2} & \tilde{\mathbf{D}}_{R_1L} & \mathbf{D}_{R_1I} \\ \mathbf{D}_{R_2R_1} & \mathbf{D}_{R_2R_2} & \tilde{\mathbf{D}}_{R_2L} & \mathbf{D}_{R_2I} \\ \tilde{\mathbf{D}}_{LR_1} & \tilde{\mathbf{D}}_{LR_2} & \tilde{\mathbf{D}}_{LL} & \tilde{\mathbf{D}}_{LI} \\ \mathbf{D}_{IR_1} & \mathbf{D}_{IR_2} & \tilde{\mathbf{D}}_{IL} & \mathbf{D}_{II} \end{bmatrix} \begin{bmatrix} \hat{\mathbf{u}}_{R_1} \\ \hat{\mathbf{u}}_{R_2} \\ \hat{\mathbf{u}}_L \\ \hat{\mathbf{u}}_I \end{bmatrix} = \begin{bmatrix} \hat{\mathbf{F}}_{R_1} \\ \hat{\mathbf{F}}_{R_2} \\ \mathbf{0} \\ \mathbf{0} \end{bmatrix} \tag{2.7}$$

Eq. (2.7) represents a reduced stiffness matrix in the steady-state. In this equation, we have to calculate the two reaction forces applied on the sleeper $\hat{\mathbf{F}}_{R_1}$ and $\hat{\mathbf{F}}_{R_2}$. We suppose that all DOF in the rail-sleeper contact surface have the same vertical displacement, hence we have:

$$\begin{cases} \forall i \in S_{R_1}\text{:} \quad \hat{\mathbf{u}}_i = \hat{\mathbf{w}}_{R_1} \quad \text{and} \quad \hat{\mathbf{F}}_{R_1} = \sum\limits_i \hat{\mathbf{F}}_{R_{1_i}} = -\hat{\mathbf{R}}_1 \\ \forall i \in S_{R_2}\text{:} \quad \hat{\mathbf{u}}_i = \hat{\mathbf{w}}_{R_2} \quad \text{and} \quad \hat{\mathbf{F}}_{R_2} = \sum\limits_i \hat{\mathbf{F}}_{R_{2_i}} = -\hat{\mathbf{R}}_2 \end{cases} \tag{2.8}$$

where S_{R_1}, $\hat{\mathbf{w}}_{R_1}$, $\hat{\mathbf{R}}_1$, S_{R_2}, $\hat{\mathbf{w}}_{R_2}$ and $\hat{\mathbf{R}}_2$ are the surface, displacement and reaction force applied on the sleeper at the rail seat 1 and 2 respectively. Therefore, if we denote d_{ik} and d_{ki} the rows and columns of the matrix DSM corresponding to $\hat{\mathbf{F}}_{R_{1_i}}$ and $\hat{\mathbf{u}}_i$ respectively, we have:

$$\hat{\mathbf{F}}_{R_{1_i}} = \sum_k d_{ik}\hat{\mathbf{u}}_k \, (\forall i \in S_{R_1}) \tag{2.9}$$

By substituting Eq. (2.9) into the Eqs. (2.8), we can rewrite :

$$-\hat{\mathbf{R}}_1 = \sum_{i \in S_{R_1}} \left(\sum_k d_{ik}\hat{\mathbf{u}}_k \right) = \sum_k \left(\sum_{i \in S_{R_1}} d_{ik} \right) \hat{\mathbf{u}}_k = \sum_k \tilde{d}_{S_{R_1}k}\hat{\mathbf{u}}_k \tag{2.10}$$

where $\tilde{d}_{S_{R_1}k} = \sum\limits_{i \in S_{R_1}} d_{ik}$. Hence, Eq (2.10) defines a new row of DSM which is the sum of all rows corresponding to the nodal force $\hat{\mathbf{F}}_{R_{1_i}}$ with $i \in S_{R_1}$. This equation deals with the contact of the rails and the sleeper. In the same way, we can have:

$$\hat{\mathbf{F}}_{R_{1_k}} = \sum_{i \notin S_{R_1}} d_{ki}\hat{\mathbf{u}}_i + \sum_{i \in S_{R_1}} d_{ki}\hat{\mathbf{u}}_i (\forall k) \tag{2.11}$$

By substituting Eq. (2.8) into Eq. (2.11) we obtain:

$$\hat{\mathbf{F}}_{R_{1_k}} = \sum_{i \notin S_{R_1}} d_{ki}\hat{\mathbf{u}}_i + \left(\sum_{i \in S_{R_1}} d_{ki} \right) \hat{\mathbf{w}}_{R_1} = \sum_{i \notin S_{R_1}} d_{ki}\hat{\mathbf{u}}_i + \tilde{d}_{kS_{R_1}}\hat{\mathbf{w}}_{R_1} \tag{2.12}$$

where $\tilde{d}_{kS_{R_1}} = \sum_{i \in S_{R_1}} d_{ki}$.

Eq. (2.12) defines a new column of DSM which is the sum of all columns corresponding to the DOF $\hat{\mathbf{u}}_i$ with $i \in S_{R_1}$. In a similar way, we can also calculate the new row $\tilde{d}_{S_{R_2}k}$ and column $\tilde{d}_{kS_{R_2}}$ of DSM which are the sum of all rows for the contact surface S_{R_2}. Thereafter, we can replace these rows and columns into Eq. (2.7) and obtain:

$$\begin{bmatrix} \mathbf{D}^*_{R_1R_1} & \mathbf{D}^*_{R_1R_2} & \tilde{\mathbf{D}}^*_{R_1L} & \mathbf{D}^*_{R_1I} \\ \mathbf{D}^*_{R_2R_1} & \mathbf{D}^*_{R_2R_2} & \tilde{\mathbf{D}}^*_{R_2L} & \mathbf{D}^*_{R_2I} \\ \tilde{\mathbf{D}}^*_{LR_1} & \tilde{\mathbf{D}}^*_{LR_2} & \tilde{\mathbf{D}}_{LL} & \tilde{\mathbf{D}}_{LI} \\ \mathbf{D}^*_{IR_1} & \mathbf{D}^*_{IR_2} & \tilde{\mathbf{D}}_{IL} & \mathbf{D}_{II} \end{bmatrix} \begin{bmatrix} \hat{\mathbf{w}}_{R_1} \\ \hat{\mathbf{w}}_{R_2} \\ \hat{\mathbf{u}}_L \\ \hat{\mathbf{u}}_I \end{bmatrix} = \begin{bmatrix} -\hat{\mathbf{R}}_1 \\ -\hat{\mathbf{R}}_2 \\ \mathbf{0} \\ \mathbf{0} \end{bmatrix} \tag{2.13}$$

By substituting the last two rows and columns of the Eq. (2.13) into the two first rows and columns, we can deduce:

$$\begin{bmatrix} \hat{\mathbf{R}}_1 \\ \hat{\mathbf{R}}_2 \end{bmatrix} = -\tilde{\mathbf{D}}_s \begin{bmatrix} \hat{\mathbf{w}}_{R_1} \\ \hat{\mathbf{w}}_{R_2} \end{bmatrix} \tag{2.14}$$

where :

$$\tilde{\mathbf{D}}_s = \mathbf{D}_{NN} - \mathbf{D}_{NM}\mathbf{D}^{-1}_{MM}\mathbf{D}_{MN} \tag{2.15}$$

with the four matrices $\mathbf{D}_{NN}$, $\mathbf{D}_{NM}$, $\mathbf{D}_{MM}$ and $\mathbf{D}_{MN}$:

$$\mathbf{D}_{NN} = \begin{bmatrix} \mathbf{D}^*_{R_1R_1} & \mathbf{D}^*_{R_1R_2} \\ \mathbf{D}^*_{R_2R_1} & \mathbf{D}^*_{R_2R_2} \end{bmatrix} \qquad \mathbf{D}_{NM} = \begin{bmatrix} \tilde{\mathbf{D}}^*_{R_1L} & \mathbf{D}^*_{R_1I} \\ \tilde{\mathbf{D}}^*_{R_2L} & \mathbf{D}^*_{R_2I} \end{bmatrix}$$

$$\mathbf{D}_{MN} = \begin{bmatrix} \tilde{\mathbf{D}}^*_{LR_1} & \tilde{\mathbf{D}}^*_{LR_2} \\ \mathbf{D}^*_{IR_1} & \mathbf{D}^*_{IR_2} \end{bmatrix} \qquad \mathbf{D}_{MM} = \begin{bmatrix} \tilde{\mathbf{D}}_{LL} & \tilde{\mathbf{D}}_{LI} \\ \tilde{\mathbf{D}}_{IL} & \mathbf{D}_{II} \end{bmatrix}$$

Now, we may also use the analytical model of periodically supported beam which permits us to obtain a relation between the sleeper displacements and reaction forces in the steady-state condition (see Appendix B):

$$\mathbf{H} \begin{bmatrix} \hat{\mathbf{R}}_1 \\ \hat{\mathbf{R}}_2 \end{bmatrix} = \begin{bmatrix} \hat{\mathbf{w}}_{R_1} \\ \hat{\mathbf{w}}_{R_2} \end{bmatrix} + \begin{bmatrix} \hat{\mathbf{w}}_{\mathcal{Q}_1} \\ \hat{\mathbf{w}}_{\mathcal{Q}_2} \end{bmatrix} \tag{2.16}$$

where the expressions of two functions $\hat{\mathbf{w}}_{\mathcal{Q}_1}$, $\hat{\mathbf{w}}_{\mathcal{Q}_2}$ are shown in Eq. (B.6).

By substituting Eq. (2.16) into Eq. (2.14), the sleeper reaction forces can be determined as follows:

$$\begin{bmatrix} \hat{\mathbf{R}}_1 \\ \hat{\mathbf{R}}_2 \end{bmatrix} = \left(\mathbf{H} + \tilde{\mathbf{D}}_s^{-1}\right)^{-1} \begin{bmatrix} \hat{\mathbf{w}}_{\mathcal{Q}_1} \\ \hat{\mathbf{w}}_{\mathcal{Q}_2} \end{bmatrix} \tag{2.17}$$

Eq. (2.17) permits us to calculate the sleeper reaction forces. Then, we can compute the model response by using eq. (2.13). Thus, this model can calculate the track responses without involving all DOF of the railway track.

September 1, 2020 9:51 IJSSD-D-20-00185

3. Numerical applications

3.1. *Comparison with analytical results*

In this example, we compare the sleeper response in the case of homogeneous foundation with the analytical model of a railway sleeper by Tran et al.[6] which is a uniform beam on a Kelvin-Voigt's foundation. For the numerical model of a uniform beam the dimensions are: 2.41 m×0.24 m×0.2m posed on an elastic foundation of dimensions: 3 m×0.6 m×0.8m.The foundation parameters are: Young's modulus E_f = 125 MPa, density 1900 kgm^{-3} and Poisson's coefficient 0.24. We note that the width of the foundation corresponds to the sleeper spacing. The mesh is generated by using a linear brick element with reduced integration (C3D8R) with: 21720 elements and 24662 nodes using ABAQUS software. The nodal displacements at the bottom foundation are fixed. The track parameters for the analytical model are given in Table 1. We calculate the sleeper responses in two cases: symmetric loads ($Q_1 = Q_2 = 100$ kN) and dis-symmetric loads ($Q_1 = 80$ kN, $Q_2 = 100$ kN).

Table 1: Parameters of the railway track

Parameters	Unit	Notation	Value
Young's modulus of rail	GPa	E_r	210
Cross-sectional moment inertia of rail	m^4	I_r	3×10^{-5}
Rail density	kgm^{-3}	ρ_r	7850
Rail section area	m^2	S_r	7.69×10^{-3}
Track gauge	m	$2a$	1.435
Stiffness of rail pad	MNm^{-1}	k_{rp}	192
Damping coefficient of rail pad	MNsm^{-1}	ζ_{rp}	1.97
Train speed	kmh^{-1}	v	150
Sleeper spacing	m	L	0.6
Young's modulus of sleeper	GPa	E_s	48
Cross-sectional moment inertia of sleeper	m^4	I_s	1.69×10^{-4}
Density of sleeper	kgm^{-3}	ρ_s	2658

Fig. 3a presents the comparison of the sleeper reaction forces by the numerical and analytical models for symmetric loads. In this case, the reaction force at the two rails are almost equal (48.35 kN for the analytical result and 48.47 kN for the numerical result). Meanwhile, the sleeper displacements from the two methods agree well (see Fig. 3b) with a maximum difference of 2.7% located at the rail seats.

The results for the dis-symmetric loads are shown in Fig. 4. The difference of the sleeper displacements at the two rail seats of the two models are 3.7% and 1.8% as shown in Fig 4b. We can conclude that the two models agree well. The small difference at the rail seat could be explained by the limit of the beam theory and the Kelvin-Voigt's foundation.

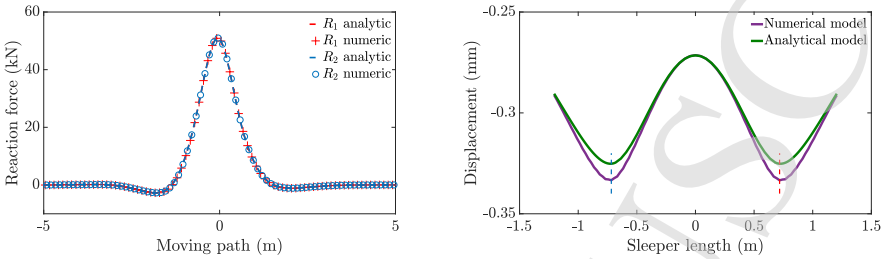

(a) Reaction force (b) Displacement

Fig. 3: Sleeper responses with symmetric loads by the analytical and numerical models

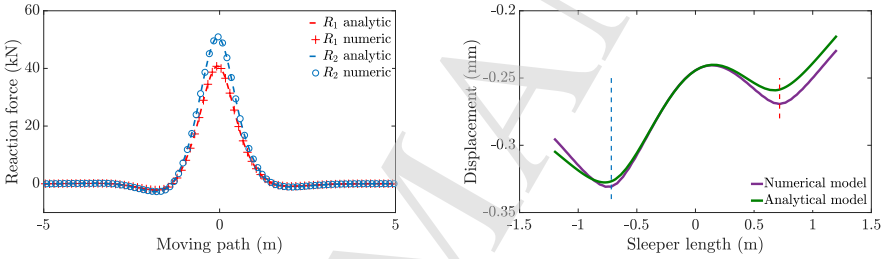

(a) Reaction force (b) Displacement

Fig. 4: Sleeper responses with dis-symmetric loads by the analytical and numerical models

3.2. *Influence of non-homogeneous foundation*

Now, we take into account the real dimensions of an M450 sleeper produced by SATEBA.

In this example, the partially consolidated foundation is modeled by 3 parts of different material parameters as shown in Fig. 5a. The evolution of the ballast can be written as 3 stages: newly tamped, partially consolidated and completely consolidated as shown in Fig 1. In this paper, the studied problem is limited to the case of non-homogeneous symmetric foundation which means that the 2 parts on the left and right have the same Young's modulus E_f meanwhile the middle part is considered more flexible than the other with Young's modulus E_m. A factor of consolidation k_c which describes the foundation behaviors is introduced as follows:

$$k_c = \frac{E_m}{E_f} \tag{3.1}$$

The value of this factor of consolidation k_c is according to the convention below:

- $k_c \ll 1$: Foundation is newly tamped (Fig. 1a).

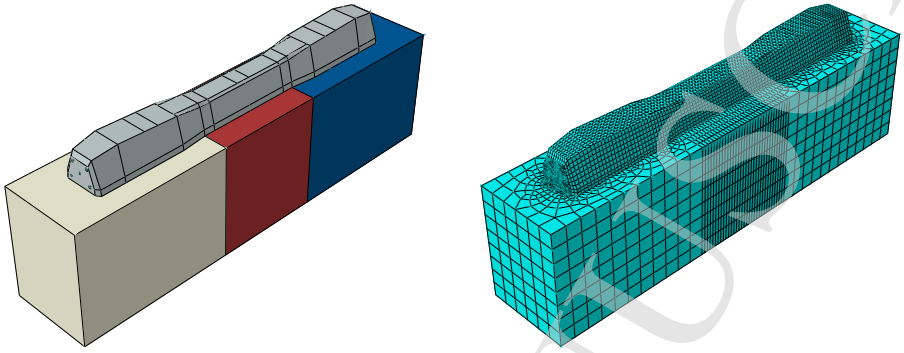

(a) Three parts of a non-homogeneous foundation (b) Mesh of the finite element model

Fig. 5: Model of an M450 sleeper on a non-homogeneous foundation

- $k_c \in [0, 1]$: Foundation is partially consolidated (Fig. 1b).
- $k_c = 1$: Foundation is completely consolidated (homogeneous) (Fig. 1c).

3.2.1. *Comparison with the homogeneous foundation*

Firstly, an example of the influence of non-homogeneous foundation on the sleeper responses will be presented with the factor $k_c = 0.3$ ($E_m = 37.5$ MPa and $E_f = 125$ MPa). The loads are dis-symmetric and the others parameters of the track are shown in Tab. 1. The mesh of the model which contains 79360 elements and 84190 nodes is shown in Fig. 5b.

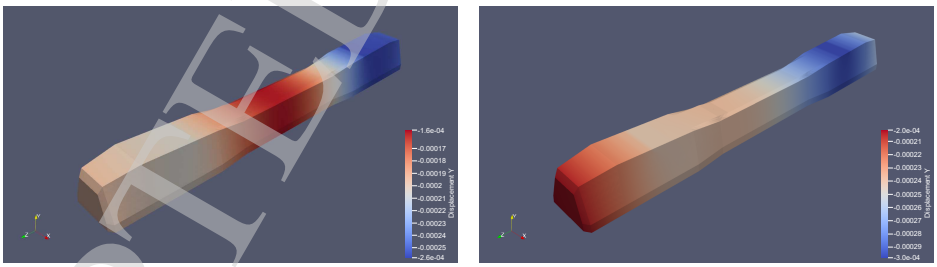

(a) Homogeneous foundation (b) Non-homogeneous foundation

Fig. 6: Comparison of sleeper displacement subjected to the dis-symmetric moving loads for the two cases of foundation

Fig. 6 shows the comparison of sleeper displacements under a dis-symmetric loads for the two cases of foundation homogeneity with the help of Paraview software (consolidated foundation (Fig. 6a) and partially consolidated foundation (Fig. 6b)).

These figures demonstrate visually the influence of the foundation state on the sleeper response.

Moreover, Fig. 7a shows that the sleeper reaction forces of the non-homogeneous foundation are smaller than the ones of the homogeneous foundation (39.55 kN and 49.68 kN at the two rail seats to compare with 40.94 kN and 51.13 kN). Meanwhile,

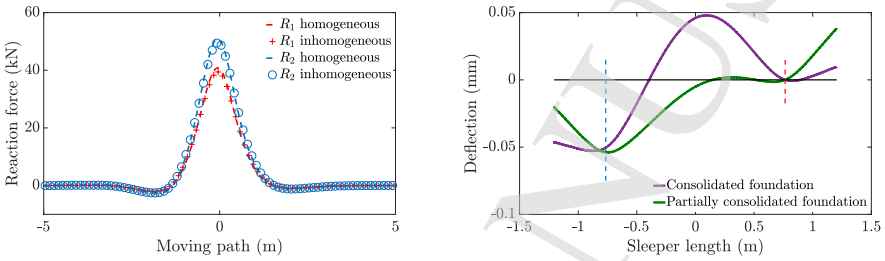

(a) Reaction force (b) Sleeper deflection

Fig. 7: Influence of the non-homogeneous foundation on the sleeper responses under dis-symmetric moving loads

the sleeper deflections are shown in the Fig. 7b. In the case of dis-symmetric loading, we see that the sleeper deforms more when the foundation is consolidated.

3.2.2. *Parametric study*

In the previous section, we see clearly that the non-homogeneous foundation influences on the sleeper responses, especially at its center. Now, we study the evolution of the sleeper strain in its lifespan by computing the track responses with different consolidation factors k_c in the interval $[0; 1]$. This work is still limited to the case of non-homogeneous symmetric foundation. We consider two cases for Young's modulus on the left and right parts: $E_f = 50$ MPa and $E_f = 175$ MPa. The Young's modulus of the middle part of the foundation E_m is given by the factor k_c via Eq. 3.1. The sleeper is subjected to symmetric moving loads.

Fig. 8 presents the sleeper strain in the longitudinal direction of the sleeper, at the distance $z_s = -42$mm from the neutral axis when the moving loads pass. The 5 lines (blue, red, green, yellow and violet) in this figure correspond respectively to the different factors: $k_c = [0.1; 0.3; 0.5; 0.7; 0.9]$. We note that the sleeper strains obtained at the rail-seats are almost unchanged. The difference of strain at the positions is 2.3%. However, the sleeper strain in the middle part is highly dependent on the consolidation of the foundation. When the foundation is newly tamped ($k_c = 0.1$), the middle part of the sleeper does not deform. The strain at the center is 0.18 μdef (for $E_f = 50$ MPa) and -4.2 μdef (for $E_f = 175$ MPa). Meanwhile, when $k_c = 0.9$ (which means that the foundation is almost homogeneous), this part is in compression with the strain at the center calculated as -28 μdef (for $E_f = 50$

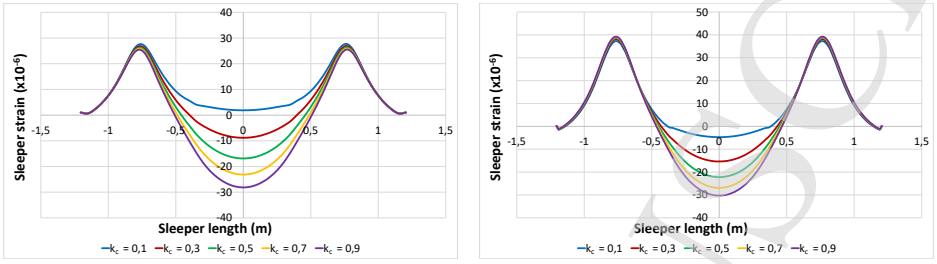

(a) $E_f = 50$ MPa (b) $E_f = 175$ MPa

Fig. 8: Influence of the factor of consolidation k_c on the sleeper strain

MPa) and -30 μdef (for $E_f = 175$ MPa).

The dependence of the sleeper strain on the consolidation of the foundation demonstrate that the middle part of the sleeper is very sensitive to the foundation state. The more consolidated the foundation is, the larger the sleeper strains are. This result shows the importance of the tamping process for the sleeper health.

4. Conclusions

A semi-analytical model for a railway track has been proposed to study the influence of the non-homogeneity of foundation on the dynamic responses of the sleepers. The ballast of this model consists of three parts with different stiffnesses. The numerical results show the difference between the sleeper responses with a homogeneous (consolidated) foundation and non-homogeneous (newly tamped and partially consolidated) foundation. Precisely, the sleeper posed on the homogeneous foundation deforms much more than the sleeper posed on the non-homogeneous foundation. In addition, a parametric study shows that the sleeper strain at the center of sleeper depends highly on the level of consolidation of the foundation. This part deforms only slightly and in tension when the track is newly tamped, meanwhile it is in compression in the case of a homogeneous foundation. This phenomenon can be used to determine the level of consolidation of the foundation from the measurement in-situ with the help of an integrated sleeper. We emphasize that this computational method considers only one track period, thus we reduce the number of track DOF which leads to a reduction of the calculation time in comparing with classical FEM.

Funding

The author(s) received no financial support for the research, authorship, and/or publication of this article.

Disclosure statement

No potential conflict of interest was reported by the authors.

Data availability statement

No data, models, or code were generated or used during the study.

Acknowledgments

This work has been developed in the context of a partnership between Sateba (Consolis Group) and École des Ponts ParisTech. The authors would like to thank the personnel of Sateba for their support.

Appendix A. Transformation of the dynamic stiffness matrix

By replacing Eq. (2.6) into the Eq. (2.4), we can get a new system of equations:

$$\begin{cases} \mathbf{D}_{R_1R_1}\hat{\mathbf{u}}_{R_1} + \mathbf{D}_{R_1R_2}\hat{\mathbf{u}}_{R_2} + \mathbf{D}_{R_1L}\hat{\mathbf{u}}_L + \mathbf{D}_{R_1R}\hat{\mathbf{u}}_L \mathrm{e}^{\left(\frac{\mathrm{i}\omega L}{v}\right)} + \mathbf{D}_{R_1I}\hat{\mathbf{u}}_I & = \hat{\mathbf{F}}_{\mathbf{R_1}} \\ \mathbf{D}_{R_2R_1}\hat{\mathbf{u}}_{R_1} + \mathbf{D}_{R_2R_2}\hat{\mathbf{u}}_{R_2} + \mathbf{D}_{R_2L}\hat{\mathbf{u}}_L + \mathbf{D}_{R_2R}\hat{\mathbf{u}}_L \mathrm{e}^{\left(\frac{\mathrm{i}\omega L}{v}\right)} + \mathbf{D}_{R_2I}\hat{\mathbf{u}}_I & = \hat{\mathbf{F}}_{\mathbf{R_2}} \\ \mathbf{D}_{LR_1}\hat{\mathbf{u}}_{R_1} + \mathbf{D}_{LR_2}\hat{\mathbf{u}}_{R_2} + \mathbf{D}_{LL}\hat{\mathbf{u}}_L + \mathbf{D}_{LR}\hat{\mathbf{u}}_L \mathrm{e}^{\left(\frac{\mathrm{i}\omega L}{v}\right)} + \mathbf{D}_{LI}\hat{\mathbf{u}}_I & = \hat{\mathbf{F}}_L \\ \mathbf{D}_{RR_1}\hat{\mathbf{u}}_{R_1} + \mathbf{D}_{RR_2}\hat{\mathbf{u}}_{R_2} + \mathbf{D}_{RL}\hat{\mathbf{u}}_L + \mathbf{D}_{RR}\hat{\mathbf{u}}_L \mathrm{e}^{\left(\frac{\mathrm{i}\omega L}{v}\right)} + \mathbf{D}_{RI}\hat{\mathbf{u}}_I & = -\hat{\mathbf{F}}_L \mathrm{e}^{\left(\frac{\mathrm{i}\omega L}{v}\right)} \\ \mathbf{D}_{IR_1}\hat{\mathbf{u}}_{R_1} + \mathbf{D}_{IR_2}\hat{\mathbf{u}}_{R_2} + \mathbf{D}_{IL}\hat{\mathbf{u}}_L + \mathbf{D}_{IR}\hat{\mathbf{u}}_L \mathrm{e}^{\left(\frac{\mathrm{i}\omega L}{v}\right)} + \mathbf{D}_{II}\hat{\mathbf{u}}_I & = \mathbf{0} \end{cases} \tag{A.1}$$

By mutiplying the 4$^{\text{th}}$ equation of the system of Eqs. (A.1) with $\mathrm{e}^{-\frac{\mathrm{i}\omega L}{v}}$, then adding its product into the 3$^{\text{rd}}$ equation of the same system of equations, we can obtain:

$$\begin{cases} \mathbf{D}_{R_1R_1}\hat{\mathbf{u}}_{R_1} + \mathbf{D}_{R_1R_2}\hat{\mathbf{u}}_{R_2} + \tilde{\mathbf{D}}_{R_1L}\hat{\mathbf{u}}_L + \mathbf{D}_{R_1I}\hat{\mathbf{u}}_I & = \hat{\mathbf{F}}_{\mathbf{R_1}} \\ \mathbf{D}_{R_2R_1}\hat{\mathbf{u}}_{R_1} + \mathbf{D}_{R_2R_2}\hat{\mathbf{u}}_{R_2} + \tilde{\mathbf{D}}_{R_2L}\hat{\mathbf{u}}_L + \mathbf{D}_{R_2I}\hat{\mathbf{u}}_I & = \hat{\mathbf{F}}_{\mathbf{R_2}} \\ \tilde{\mathbf{D}}_{LR_1}\hat{\mathbf{u}}_{R_1} + \tilde{\mathbf{D}}_{LR_2}\hat{\mathbf{u}}_{R_2} + \tilde{\mathbf{D}}_{LL}\hat{\mathbf{u}}_L + \tilde{\mathbf{D}}_{LI}\hat{\mathbf{u}}_I & = \mathbf{0} \\ \mathbf{D}_{IR_1}\hat{\mathbf{u}}_{R_1} + \mathbf{D}_{IR_2}\hat{\mathbf{u}}_{R_2} + \tilde{\mathbf{D}}_{IL}\hat{\mathbf{u}}_L + \mathbf{D}_{II}\hat{\mathbf{u}}_I & = \mathbf{0} \end{cases} \tag{A.2}$$

where :

$$\begin{cases} \tilde{\mathbf{D}}_{LL} = \mathbf{D}_{LL} + \mathbf{D}_{LR}\mathrm{e}^{\left(\frac{\mathrm{i}\omega L}{v}\right)} + \mathbf{D}_{RL}\mathrm{e}^{\left(-\frac{\mathrm{i}\omega L}{v}\right)} + \mathbf{D}_{RR} \\ \tilde{\mathbf{D}}_{LR_1} = \mathbf{D}_{LR_1} + \mathbf{D}_{RR_1}\mathrm{e}^{\left(-\frac{\mathrm{i}\omega L}{v}\right)}, \quad \tilde{\mathbf{D}}_{R_1L} = \mathbf{D}_{R_1L} + \mathbf{D}_{R_1R}\mathrm{e}^{\left(\frac{\mathrm{i}\omega L}{v}\right)} \\ \tilde{\mathbf{D}}_{LR_2} = \mathbf{D}_{LR_2} + \mathbf{D}_{RR_2}\mathrm{e}^{\left(-\frac{\mathrm{i}\omega L}{v}\right)}, \quad \tilde{\mathbf{D}}_{R_2L} = \mathbf{D}_{R_2L} + \mathbf{D}_{R_2R}\mathrm{e}^{\left(\frac{\mathrm{i}\omega L}{v}\right)} \\ \tilde{\mathbf{D}}_{LI} = \mathbf{D}_{LI} + \mathbf{D}_{RI}\mathrm{e}^{\left(-\frac{\mathrm{i}\omega L}{v}\right)}, \quad \tilde{\mathbf{D}}_{IL} = \mathbf{D}_{IL} + \mathbf{D}_{IR}\mathrm{e}^{\left(\frac{\mathrm{i}\omega L}{v}\right)} \end{cases} \tag{A.3}$$

Appendix B. Periodically supported beam model

The periodically supported beam is shown in Fig. 9.

When the rails are modeled by periodically supported beams, Hoang et al.[5,15] demonstrated a relation between the reaction force $\hat{\mathbf{R}}_k(\omega)$ on each rail k and the rail displacement in the frequency domain. This relation is developed for two types

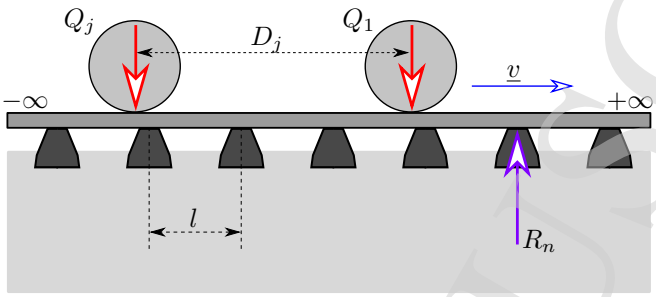

Fig. 9: Periodically supported beam model

of beam model for the rail: Euler-Bernoulli's beam, and Timoshenko's beam and it is written as follows:

$$\hat{\mathbf{R}}_k(\omega) = \mathcal{K}(\omega)\hat{\mathbf{w}}_r^{[k]}(\omega) + \mathcal{Q}_k(\omega) \tag{B.1}$$

where $\hat{\mathbf{w}}_r^{[k]}$ are displacements of the rail k at the sleeper position ($k \in [1, 2]$). The constants $\mathcal{K}(\omega)$, $\mathcal{Q}_k(\omega)$ are the equivalent stiffness and the equivalent charges of the two rails respectively which are determined in the case of the Euler-Bernoulli's beam model as follows:

$$\begin{cases} \mathcal{K}(\omega) & = 4\lambda_r^3 E_r I_r \left[\dfrac{\sin l\lambda_r}{\cos l\lambda_r - \cos\frac{\omega l}{v}} - \dfrac{\sinh l\lambda_r}{\cosh l\lambda_r - \cos\frac{\omega l}{v}} \right]^{-1} \\ \mathcal{Q}_k(\omega) & = \dfrac{\mathcal{K}(\omega)}{vE_r I_r \left[\left(\frac{\omega}{v}\right)^4 - \lambda_r^4 \right]} \displaystyle\sum_{j=1}^{K} Q_j^{[k]} \mathrm{e}^{\mathrm{i}\omega\frac{D_j}{v}} \end{cases} \tag{B.2}$$

where $\lambda_r = \sqrt[4]{\frac{\rho_r S_r \omega^2}{E_r I_r}}$. The parameters E_r, I_r, ρ_r, S_r are the Young's modulus, cross-sectional inertial, density, cross-sectional area of rail respectively and l is the track gauge. The moving load parameters are characterized by the train speed v, the vertical loads on each rail $Q_j^{[k]}$, the wheel number K and the wheel positions D_j. We remark that the equivalent stiffness $\mathcal{K}(\omega)$ depends only on the rail parameters and the moving forces.

Let $\hat{\mathbf{w}}_{R_k}(\omega)$ be the sleeper displacement in the frequency domain at two rail seats positions $x = \pm a$ of the sleeper, the forces $\hat{\mathbf{R}}_k(\omega)$ can be expressed by the constitutive law of the rail pads in the frequency domain as follows:

$$\hat{\mathbf{R}}_k(\omega) = -k_p \left(\hat{\mathbf{w}}_r^{[k]}(\omega) - \hat{\mathbf{w}}_{R_k}(\omega) \right) \tag{B.3}$$

where $k_p = k_{rp} + \mathrm{i}\omega\zeta_{rp}$ is the dynamic stiffness of the rail pad and k_{rp}, ζ_{rp} are the stiffness, damping coefficients of the rail pads respectively. By substituting Eq. (B.1) into Eq. (B.3), we obtain:

$$\hat{\mathbf{R}}_k(\omega) = \frac{k_p \mathcal{K}}{k_p + \mathcal{K}} \hat{\mathbf{w}}_{R_k}(\omega) + \frac{k_p}{k_p + \mathcal{K}} \mathcal{Q}_k(\omega) \tag{B.4}$$

Eq. (B.4) can be also expressed in the other form:

$$\eta_{\mathcal{K}}\hat{\mathbf{R}}_k = \hat{\mathbf{w}}_{R_k} + \hat{\mathbf{w}}_{\mathcal{Q}_k} \tag{B.5}$$

where the two functions $\eta_{\mathcal{K}}$ and $\hat{\mathbf{w}}_{\mathcal{Q}_k}$ are calculated as follows:

$$\begin{cases} \eta_{\mathcal{K}} = \dfrac{k_p + \mathcal{K}}{k_p \mathcal{K}} \\ \hat{\mathbf{w}}_{\mathcal{Q}_k} = \dfrac{1}{vE_rI_r\left[\left(\dfrac{\omega}{v}\right)^4 - \lambda^4\right]} \displaystyle\sum_{j=1}^{K} Q_j^{[k]} \mathrm{e}^{-\mathrm{i}\omega\frac{D_j}{v}} \end{cases} \tag{B.6}$$

References

1. AEA Technology, Design of mono block concrete sleepers, UIC leaflet 713 R AEATR-TCE-2001-336 Issue 0, European Railway Research Institute (2002).
2. L. Fryba, *Vibration of solids and structures under moving load* (Thomas Telford, 1972).
3. V.-H. Nguyen and D. Duhamel, Finite element procedures for nonlinear structures in moving coordinates. Part 1: Infinite bar under moving axial loads, *Computers & Structures* **84**(21) (2006) 1368–1380.
4. V.-H. Nguyen and D. Duhamel, Finite element procedures for nonlinear structures in moving coordinates. Part II: Infinite beam under moving harmonic loads, *Computers & Structures* **86**(21) (2008) 2056–2063.
5. T. Hoang, D. Duhamel and G. Foret, Dynamical response of a Timoshenko beams on periodical nonlinear supports subjected to moving forces, *Engineering Structures* **176** (dec 2018) 673–680.
6. L.-H. Tran, T. Hoang, F. Gilles, D. Duhamel, S. Messad and A. Loaëc, A fast analytic method to calculate the dynamic response of railways sleepers, *Journal of Vibration and Acoustics* **141**(1) (2019).
7. L.-H. Tran, T. Hoang, F. Gilles, D. Duhamel, S. Messad and A. Loaëc, Analytical model of the dynamics of railway sleeper, in *6th International Conference on Computational Methods in Structural Dynamics and Earthquake (COMPDYN)* (Rhodes, Greece, 2017), pp. 3937–3948.
8. D. Mead, Free wave propagation in periodically supported, infinite beams, *Journal of Sound and Vibration* **11** (feb 1970) 181–197.
9. D. Mead, Wave propagation in continuous periodic structures : Research contributions from Southampton, 1964-1995, *Journal of Sound and Vibration* **190**(3) (1996) 495–524.
10. A. Nordborg, Vertical rail vibrations: parametric exication, *Acustica* **84** (1998) 289–300.
11. X. Sheng, C. Jones and D. Thompson, Responses of infinite periodic structures to moving or stationary harmonic loads, *Journal of Sound and Vibration* **282**(1) (2005) 125–149.
12. H. Ding, L.-Q. Chen and S.-P. Yang, Convergence of Galerkin truncation for dynamic response of finite beams on nonlinear foundations under a moving load, *Journal of Sound and Vibration* **331**(10) (2012) 2426–2442.
13. J. Sadeghi and M. Fesharaki, Importance of nonlinearity of track support system in modeling of railway track dynamics, *International Journal of Structural Stability and Dynamics* **13**(01) (2013) p. 1350008.

September 1, 2020 9:51 IJSSD-D-20-00185

14. L. Morino, J. W. Leech and E. A. Witmer, Optimal predictor-corrector method for systems of second-order differential equations, *AIAA Journal* **12**(10) (1974) 1343–1347.
15. T. Hoang, D. Duhamel, G. Foret, H.-P. Yin and G. Cumunel, Response of a periodically supported beam on a nonlinear foundation subjected to moving loads, *Nonlinear Dynamics* **86** (Oct 2016) 953–961.
16. X. Yang, Y. Shu and S. Zhou, An explicit periodic nonlinear model for evaluating dynamic response of damaged slab track involving material nonlinearity of damage in high speed railway, *Construction and Building Materials* **168** (apr 2018) 606–621.
17. Z. Dimitrovová and J. Varandas, Critical velocity of a load moving on a beam with a sudden change of foundation stiffness: Applications to high-speed trains, *Computers & Structures* **87**(19) (2009) 1224 – 1232, Civil-Comp Special Issue.
18. J. N. Varandas, P. Hölscher and M. A. Silva, Dynamic behaviour of railway tracks on transitions zones, *Computers & Structures* **89**(13) (2011) 1468 – 1479.
19. A. Paixão, E. Fortunato and R. Calçada, Transition zones to railway bridges: Track measurements and numerical modelling, *Engineering Structures* **80** (2014) 435 – 443.
20. Y. S. Wu, Y. B. Yang and J. D. Yau, Three-dimensional analysis of train-rail-bridge interaction problems, *Vehicle System Dynamics* **36**(1) (2001) 1–35.
21. A. Paixão, J. N. Varandas, E. Fortunato and R. Calçada, Numerical simulations to improve the use of under sleeper pads at transition zones to railway bridges, *Engineering Structures* **164** (2018) 169 – 182.
22. C. Alves Ribeiro, A. Paixão, E. Fortunato and R. Calçada, Under sleeper pads in transition zones at railway underpasses: numerical modelling and experimental validation, *Structure and Infrastructure Engineering* **11**(11) (2015) 1432–1449.
23. S. Kaewunruen, T. Lewandrowski and K. Chamniprasart, Dynamic responses of interspersed railway tracks to moving train loads, *International Journal of Structural Stability and Dynamics* **18**(01) (2018) p. 1850011.
24. J. Dai, K. K. Ang, D. Jiang, V. H. Luong and M. T. Tran, Dynamic response of high-speed train-track system due to unsupported sleepers, *International Journal of Structural Stability and Dynamics* **18**(10) (2018) p. 1850122.
25. X. Xiao and W.-X. Ren, A versatile 3d vehicle-track-bridge element for dynamic analysis of the railway bridges under moving train loads, *International Journal of Structural Stability and Dynamics* **19**(04) (2019) p. 1950050.
26. Q. Xie, Y. X. Zhou, Y. Zhan, K. Y. Sze and W. S. Han, A comparative study on the beam and continuum finite element models for the rail–wheel vibration, *International Journal of Structural Stability and Dynamics* **19**(07) (2019) p. 1950076.
27. S. Grassie, Dynamic modelling of concrete railway sleepers, *Journal of Sound and Vibration* **187** (nov 1995) 799–813.
28. G. Kumaran, D. Menon and K. Kríhnan Nair, Evaluation of dynamic load on rail track sleepers based on vehicle-track modeling and analysis, *International Journal of Structural Stability and Dynamics* **02**(03) (2002) 355–374.
29. S. Kaewunruen and A. M. Remennikov, Effect of improper ballast packing/tamping on dynamic behaviors of on-track railway concrete sleeper, *International Journal of Structural Stability and Dynamics* **7**(1) (2007) 167–177.
30. S. Kaewunruen and A. M. Remennikov, Nonlinear transient analysis of a railway concrete sleeper in a track system, *International Journal of Structural Stability and Dynamics* **08**(03) (2008) 505–520.
31. R. Gustavson and K. Gylltoft, Infuence of cracked sleepers on the global track response: Coupling of a linear track model and nonlinear finite element analyses, *Proceedings of the Institution of Mechanical Engineers, Part F: Journal of Rail and Rapid*

Transit **216**(1) (2002) 41–51.

32. J. F. Ruiz, P. A. Costa, R. Calçada, L. E. M. Rodríguez and A. Colaço, Study of ground vibrations induced by railway traffic in a 3d fem model formulated in the time domain: experimental validation, *Structure and Infrastructure Engineering* **13**(5) (2017) 652–664.
33. T. Hoang, D. Duhamel, G. Foret and P. Jean-Luc, Computational method for the dynamics of railway tracks on a non-uniform viscoelastic foundation, *Procedia Engineering* **199** (2017) 354 – 359, X International Conference on Structural Dynamics, EURODYN 2017.
34. T. Hoang, D. Duhamel, G. Foret, H. Yin, P. Joyez and R. Caby, Calculation of force distribution for a periodically supported beam subjected to moving loads, *Journal of Sound and Vibration* **388** (2017) 327–338.